

# Luttinger parameters and momentum distribution function for the half-filled spinless fermion Holstein model: A DMRG approach

S. EJIMA and H. FEHSKE

*Institut für Physik, Ernst-Moritz-Arndt-Universität Greifswald, 17489 Greifswald, Germany*

PACS 71.10.Hf – Non-Fermi-liquid ground states, electron phase diagrams and phase transitions in model systems

PACS 71.38.-k – Polarons and electron-phonon interactions

**Abstract.** - We reexamine the nature of the metallic phase of the one-dimensional half-filled Holstein model of spinless fermions. To this end we determine the Tomonaga-Luttinger-liquid correlation parameter  $K_\rho$  by large-scale density-matrix renormalisation-group (DMRG) calculations, exploiting (i) the leading-order scaling relations between the ground-state energy and the single-particle excitation gap and (ii) the static charge structure factor in the long-wavelength limit. While both approaches give almost identical results for intermediate-to-large phonon frequencies, we find contrasting behaviour in the adiabatic regime: (i)  $K_\rho > 1$  (attractive) versus (ii)  $K_\rho < 1$  (repulsive). The latter result for the correlation exponent is corroborated by data obtained for the momentum distribution function  $n(k)$ , which puts the existence of an attractive metallic state in the spinless fermion Holstein model into question. We conclude that the scaling relation must be modified in the presence of electron-phonon interactions with noticeable retardation.

During the last three decades we have seen a constant growth of experimental realizations of one-dimensional (1D) materials. Nowadays the progress in nanotechnology allows to manufacture isolated carbon nanotubes or quantum wires [1]. But there are also bulk materials with quasi-1D structures inside. Famous examples are conjugated polymers, charge transfer salts, halogen-bridged transition metal complexes, ferroelectric perovskites, spin Peierls compounds, molecular metals or organic superconductors [2]. The apparent diversity of physical properties observed for different material classes has its seeds in the strong competition between the itinerancy of the electronic charge carriers on the one hand and the electron-electron and electron-lattice interactions on the other hand. The latter tend to establish insulating spin-density-wave or charge-density-wave (CDW) ground states, respectively, at least for commensurate band fillings [3–8]. Interactions have drastic effects in 1D systems compared to higher dimensions. Most notably one observes a “collectivisation” of any excitation. As a consequence, for fermionic systems, the usual Fermi liquid description breaks down [9]. Luttinger liquid theory provides an adequate compensation [10]. It tells us that all ground-state, spectral and thermodynamic properties of a Luttinger liquid are basically controlled by a few (non-universal) pa-

rameters. This result can be used in the following way. Starting from a specific microscopic model, one can try to compute certain (thermodynamic) quantities exactly, e.g. for finite systems by elaborate numerical techniques, and afterwards extract the Luttinger liquid parameters, e.g. the charge correlation exponent  $K_\rho$  and charge velocity  $u_\rho$ , out of them. Advantageously these parameters, describing the overall low-energy physics of our system, are much less sensitive to finite-size effects than the correlation functions themselves. Of course, the concept of a Luttinger liquid has to be taken as a starting point to study more complex situations, comprising e.g. the lattice degrees of freedom or disorder effects. Then the Luttinger parameters become effective parameters, which characterise very basic properties of the system, such as an attractive ( $K_\rho > 1$ ) or repulsive ( $K_\rho < 1$ ) interaction between the particles [9,11].

In this respect, focusing on the coupling of charge carriers to the vibrations of a deformable lattice, the so-called Holstein model of spinless fermions (HMSF) [12],

$$\begin{aligned} \mathcal{H} = & -t \sum_j \left( c_j^\dagger c_{j+1} + \text{h.c.} \right) + \omega_0 \sum_j b_j^\dagger b_j \\ & - g \omega_0 \sum_j \left( b_j^\dagger + b_j \right) \left( n_j - \frac{1}{2} \right), \end{aligned} \quad (1)$$

is particularly rewarding to study. It accounts for a tight-binding electron band ( $\propto t$ ), a local electron-phonon (EP) interaction ( $\propto g$ ), and the energy of the phonon subsystem in harmonic approximation. In eq. (1),  $c_j^\dagger$  ( $c_j$ ) creates (annihilates) an electron at Wannier site  $j$  of a 1D lattice with  $N$  sites,  $b_j^\dagger$  ( $b_j$ ) are the corresponding bosonic operators for a dispersionless optical phonon, and  $\omega_0$  is the frequency of such an internal (e.g. molecular) vibration.

Despite its seemingly simplicity, the 1D HMSF is not exactly solvable. It is generally accepted, however, that the model exhibits a quantum phase transition from a metal to a CDW insulator at half-filling, when the EP coupling  $g$  increases at fixed  $\omega_0 > 0$ .<sup>1</sup> The CDW phase above  $g_c(\omega_0)$  is connected to a (Peierls) distortion of the lattice, and can be classified as traditional band insulator and polaronic superlattice, respectively, in the adiabatic ( $\omega_0 \ll 1$ ) and anti-adiabatic ( $\omega_0 \gg 1$ ) regimes [13,14]. A wide range of analytical and numerical methods have been applied to map out the phase diagram of the HMSF in the whole  $g - \omega_0$  plane [13,15–19], with significant differences in the region of small-to-intermediate phonon frequencies. The results agree in the anti-adiabatic strong EP coupling limit ( $\omega_0 \rightarrow \infty$ ,  $g > 1$ ), where the HMSF possesses XXZ-model physics. There a Kosterlitz-Thouless type transition [20] occurs at the spin isotropy point, with  $K_\rho$  reaching  $1/2$  from above at the transition point [15,18].

In the first instance, however, the correlation exponent  $K_\rho$  can be used to characterise the metallic phase itself. According to Haldane’s conjecture [21], a 1D gapless (metallic) system of interacting fermions should belong to the Tomonaga-Luttinger liquid (TLL) universality class [10,22]. For a TLL of spinless fermions, the ground-state energy  $E(N)$  and the one-particle charge excitation gap  $\Delta_{c_1}$  of a finite system with  $N$  sites scale to leading order as [11,23]:

$$\frac{E(N)}{N} = \varepsilon(\infty) - \frac{\pi}{3} \frac{u_\rho}{2} \frac{1}{N^2}, \quad (2)$$

$$\Delta_{c_1} = E^\pm(N) - E(N) = \pi \frac{u_\rho}{2} \frac{1}{K_\rho N}. \quad (3)$$

Here,  $\varepsilon(\infty)$  denotes the energy density of the infinite system with  $N/2$  electrons,  $E^\pm(N)$  are the ground-state energies with  $\pm 1$  fermion away from half filling, and  $u_\rho$  is the renormalised charge velocity.<sup>2</sup> Using these equations from field theory, in the past,  $K_\rho$  and  $u_\rho$  were determined for the HMSF on finite clusters by various exact numerical techniques [13,17,18,26]. Interestingly the TLL phase seems to split into two different regions: For large phonon frequencies the effective fermion-fermion interaction is repulsive ( $K_\rho < 1$ ), while it is attractive ( $K_\rho > 1$ ) for small frequencies [13,26]. In the former (anti-adiabatic) regime

<sup>1</sup>We consider the half-filled band case hereafter, i.e.,  $\frac{1}{N} \sum_j \langle c_j^\dagger c_j \rangle = \frac{1}{2}$ , and take  $t = 1$  as energy unit.

<sup>2</sup>The TLL scaling relations (2) and (3) were also derived for spinful systems [24], and e.g. used in order to compute the central charge in the framework of the  $t$ - $J$  model [25].

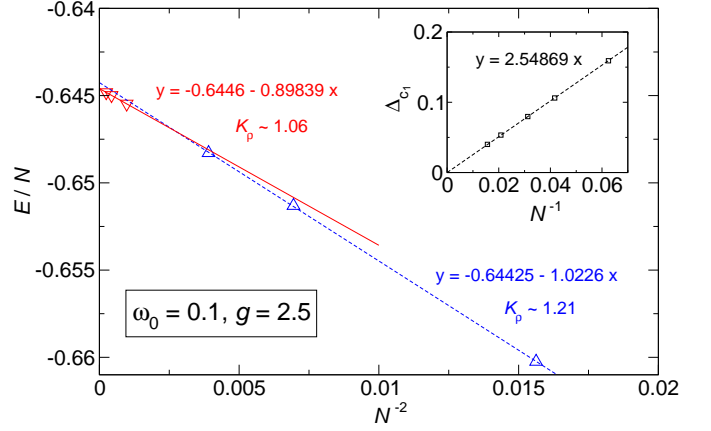


Fig. 1: (Colour online) Finite-size scaling of the ground-state energy  $E(N)$  and the one-particle charge excitation gap  $\Delta_{c_1}$  (inset) in the spinless Holstein model at half filling. Results are obtained by DMRG for  $\omega_0 = 0.1$  and  $g = 2.5$ . The linear equations give the coefficients of a straight-line fit to the scaling relations (2) and (3).

the kinetic energy ( $\propto u_\rho$ ) is strongly reduced and the charge carriers behave like (small) polarons [27,28]. By contrast the mass renormalisation is rather weak in the adiabatic regime [26]. The size of the phonon frequency also significantly affects the electron and phonon spectral functions [14,19,29].

The existence of an attractive TLL ( $K_\rho > 1$ ) in the HMSF is by no means obvious however. Although retardation effects might lead to an effective attraction between electrons at small  $\omega_0/t$  (i.e., a second electron may take the advantage of the lattice distortion left by the first one), it has been pointed out that such an interaction is ineffective in the case of spinless fermions for small EP couplings because of the Pauli exclusion principle [15].<sup>3</sup> Furthermore, if  $K_\rho$  would increase with increasing EP coupling at small  $\omega_0$ , as indicated by different numerical studies [13,26] exploiting equations (2) and (3), how could we detect the phase transition from  $K_\rho \rightarrow 1/2$  in the adiabatic regime? Of course, equations (2) and (3) are leading-order expressions only, and nonlinear correction terms have to be taken into account in order to obtain accurate data for  $g_c$  [18]. This particularly applies to the adiabatic region. According to table III in Ref. [18] the difference between the  $g_c$  determined with and without nonlinear correction terms adds up to more than 3% for  $\omega_0 = 0.1$ , whereas it is only 0.4% for  $\omega_0 = 10$ . Actually the charge velocity  $u_\rho$  depends strongly on the system’s size as shown in figure 1 obtained by a density matrix renormalisation group (DMRG) calculation. Extrapolating the ground-state energies  $E(N)$  for  $N = 8, 12$  and  $16$ , the charge velocity  $u_\rho$  can be estimated as  $u_\rho/2 \sim 0.977$ , so that  $K_\rho \sim 1.21$  from the finite-size scaling of  $\Delta_{c_1}$ , while taking the ground-state energies for  $N = 32, 48$  and  $64$ , the extracted value of  $K_\rho$  reduces to  $1.06$  ( $u_\rho/2 \sim 0.858$ ). Moreover we are faced

<sup>3</sup>Note this argument does not hold for the spinful Holstein model.

with the difficulty that the single particle excitation gap seems to scale to zero (see inset of figure 1 for  $\omega_0 = 0.1$ ,  $g = 2.5$ ), i.e.  $\Delta_{c1}$  gives no signal for a pairing instability. Because of this situation it is highly desirable to find a reliable and numerical efficient method for calculating the correlation exponent  $K_\rho$  with high precision in the whole TLL regime.

Recently Ejima *et al.* [30] have shown that  $K_\rho$  can be determined for fermionic models accurately in an alternative way: By a DMRG calculation of the charge structure factor for systems with open boundary conditions. The approach was extended to coupled fermion-boson systems and has been used, e.g., to analyse the metal-insulator transition points in a model with boson affected transport, for both small and large boson frequencies [31].

In this work we adapt this calculation scheme to the 1D Holstein model of spinless fermions (1) and reexamine, in particular, the possible existence of a metallic phase with attractive interaction. To this end we compute, in a first step, the static charge structure factor

$$S_c(q) = \frac{1}{N} \sum_{j,l} e^{iq(j-l)} \left\langle \left( c_j^\dagger c_j - \frac{1}{2} \right) \left( c_l^\dagger c_l - \frac{1}{2} \right) \right\rangle, \quad (4)$$

and extract, in a second step, the TLL correlation exponent  $K_\rho$ , being proportional to the slope of  $S_c(q)$  in the long-wavelength limit [7, 30, 32]:

$$K_\rho = \pi \lim_{q \rightarrow 0^+} \frac{S_c(q)}{q}, \quad q = \frac{2\pi}{N}, \quad N \rightarrow \infty. \quad (5)$$

Moreover we calculate the momentum distribution function for the HMSF and, having accurate data for  $K_\rho$  at hand, analyse the results within a TLL description, also in relation to the corresponding results for the half-filled spinless  $t$ - $V$  model. When treating coupled 1D fermion-boson systems by DMRG we employ the pseudo-site approach [33] which maps a bosonic site, containing  $2^{n_b}$  states, exactly to  $n_b$  pseudo-sites. For the numerics presented below we have taken into account up to  $n_b = 5$  pseudo-sites, so that the  $n_b$ -th local boson density is always smaller than  $10^{-8}$ . In addition we kept  $m = 1200$  density-matrix eigenstates. Then the discarded weight was always smaller than  $1.0 \times 10^{-10}$ .

Figure 2 (a) presents  $K_\rho$  obtained from eq. (5) for various phonon frequencies. Note that data points in (a) represent  $K_\rho$ -values extrapolated to the infinite system at fixed  $(g, \omega_0)$  [cf., e.g., panel (c)]. For intermediate-to-large phonon frequencies we find  $K_\rho(g) < 1$  for all  $g$ , but an appreciable reduction of  $K_\rho$  takes place above  $g = 1$  only. The strong decrease of  $K_\rho$  and  $u_\rho$  (not shown) for  $g > 1$  is closely connected to polaron formation, which appears at about  $g \simeq 1$  in the non-to-anti-adiabatic regime [28]. There the TLL typifies a (repulsive) polaronic metal [14]. We emphasise that in this frequency region the values of  $K_\rho$ , computed from eq. (5) via the static charge structure factor, reasonably agree with those determined by the scaling relations (2), (3) [see panel (a), filled and open

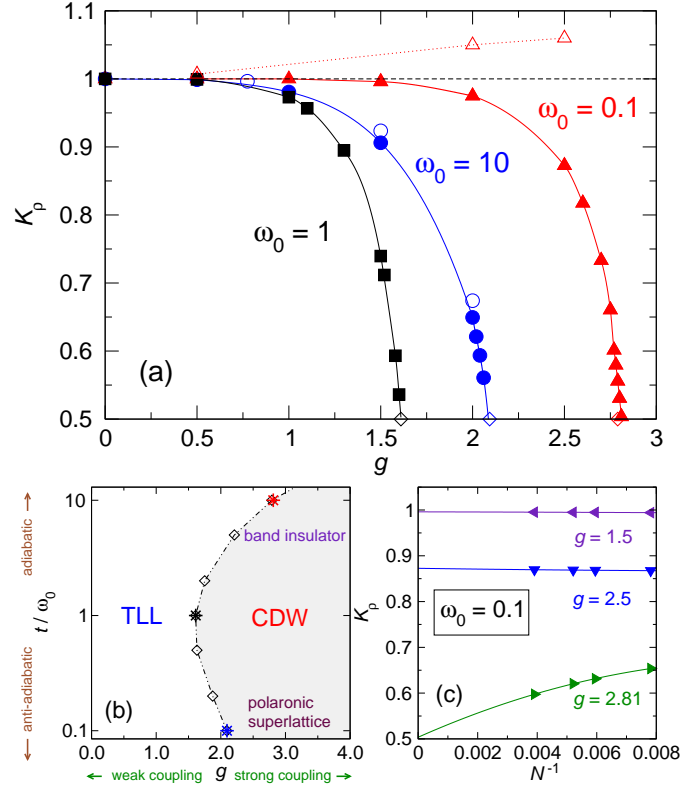


Fig. 2: (Colour online) Panel (a): TLL parameter  $K_\rho$  in the spinless Holstein model at half filling. Closed symbols are obtained via  $S_c(q)$  from eq. (5) for  $\omega_0 = 0.1$  (triangles), 1 (squares), and 10 (circles).  $K_\rho$  obtained from the scaling relations (2) and (3) are included as open symbols. Lines are guides to the eye. Panel (b): Ground-state phase diagram of the 1D half-filled spinless Holstein model according to Refs. [13, 14, 18]. Stars denote the phase transition points obtained from  $K_\rho = 1/2$  in (a). Panel (c):  $K_\rho$  as a function of the inverse system size at various EP couplings  $g = 1.5, 2.5$ , and 2.81 for  $\omega_0 = 0.1$  (adiabatic regime). Lines are polynomial fits.

symbols for  $\omega_0 = 10$ ]. Furthermore, our values for the critical coupling,  $g_c$ , confirm previous results (although a Kosterlitz-Thouless transition is difficult to detect because the gap opens exponentially slow), as can be seen by inserting the points where  $K_\rho(g_c) = 1/2$  (stars) into the existing phase diagram of the HMSF [13, 14, 18] [cf. panel (b)].

Let us now look whether the situation changes when the phonon frequency becomes smaller, i.e., when we enter the adiabatic regime. Figure 2 (c) shows the scaling of  $K_\rho$  at  $\omega_0 = 0.1$ , based on the relation (5), for up to  $N = 256$  sites, using open boundary conditions. The lines are second-order polynomial fits. Surprisingly, we find that  $K_\rho$  scales to values smaller than unity for any EP coupling (filled symbols). This holds for other adiabatic phonon frequencies  $\omega_0 < 1$  as well. Taking this result seriously, we arrive at the conclusion that the HMSF does not exhibit a metallic TLL phase with attractive interaction,

which is in strong contradiction to the reasonings based on the leading-order energy scaling laws (2) and (3) [see open symbols in figure 2 (a)]. We would like to point out, however, that our  $S_c(q)$ -based approach gives apparently the correct value of the critical coupling for the TLL-CDW metal-insulator transition in the adiabatic HMSF. In previous work,  $g_c$  was estimated as  $g_c(\omega_0 = 0.1) \sim 2.8$  [18], which is in accordance with our DMRG-results for  $K_\rho(N)$  at  $g = 2.81$  that clearly extrapolate to  $K_\rho = 1/2$  in the thermodynamic limit. This means that the TLL-CDW transition at small  $\omega_0 = 0.1$  seems to be of Kosterlitz-Thouless type as well.

To substantiate these findings, we investigate another quantity of interest, the so-called momentum distribution function,

$$n(k) = \frac{1}{N} \sum_{j,l} e^{ik(j-l)} \langle c_j^\dagger c_l \rangle. \quad (6)$$

Basically  $n(k)$  is the Fourier transform of the equal time Green's function [9] and therefore gives the occupation of fermionic states carrying momentum  $k$ . For free fermions, at  $T = 0$ , all states up to the Fermi energy,  $E_F$ , are occupied, so that  $n(k)$  has a discontinuity ( $Z = 1$ ) at the corresponding Fermi momentum  $k_F$ .<sup>4</sup> For a 1D TLL, instead of the (Fermi liquid archetypical) jump of  $n(k)$  at  $k_F$ , one finds an essential power law singularity, corresponding to a vanishing quasiparticle weight  $Z = 0$ ,

$$n(k) = n_{k_F} - C|k - k_F|^\alpha \text{sgn}(k - k_F), \quad (7)$$

where  $n_{k_F} = 1/2$  for the half-filled band case. For spinless fermions, again the critical exponent  $\alpha$  is given by the TLL parameter  $K_\rho$  :

$$\alpha = \frac{1}{2}(K_\rho + K_\rho^{-1}) - 1. \quad (8)$$

The relation (7) with (8) was first derived in [10,34], and afterwards many analytical [35] and numerical [36] calculations were performed in order to determine the momentum distribution in the weak and strong coupling regimes. By means of DMRG,  $n(k)$  can be computed directly from the Fourier transformed  $\langle c_j^\dagger c_l \rangle$  correlator,  $n(k) = \frac{1}{N} \sum_{j,l=1}^N \cos(k(j-l)) \langle c_j^\dagger c_l \rangle$ , where  $k = \frac{2\pi}{N}m$  with  $m = 0, \dots, N/2$ . In the following, we calculate  $n(k)$  for a linear chain with periodic boundary conditions, and  $N = 66$  sites.

Before we discuss  $n(k)$  for the HMSF, let us consider a somewhat simpler, purely fermionic model, however, the spinless  $t$ - $V$  model,

$$\mathcal{H} = -t \sum_j \left( c_j^\dagger c_{j+1} + \text{h.c.} \right) + V \sum_j n_j n_{j+1}, \quad (9)$$

where  $V$  is the nearest neighbour Coulomb interaction. This is of avail because the  $t$ - $V$  model can also be mapped

<sup>4</sup>In an interacting Fermi liquid system there is still a discontinuity, but  $Z < 1$ .

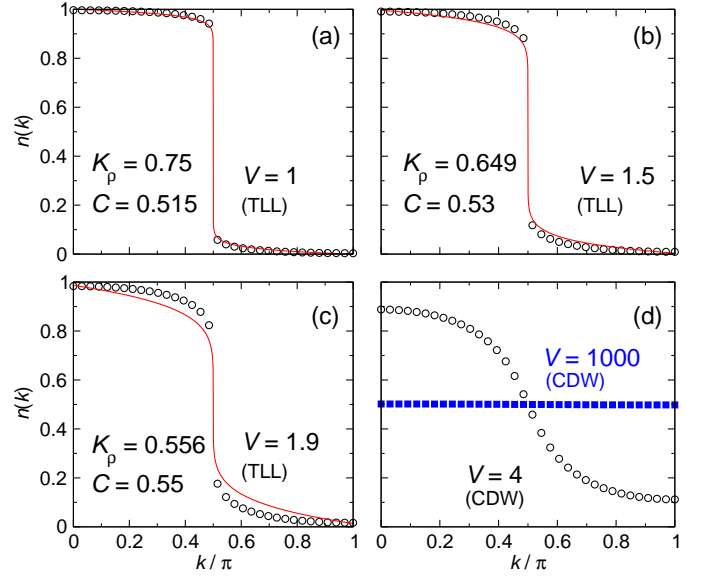


Fig. 3: (Colour online) Momentum distribution function  $n(k)$  for the half-filled spinless  $t$ - $V$  model. Lines are fit to eq. (7) with  $K_\rho$  taken from eq. (10).

onto the exactly solvable XXZ-Heisenberg model (i.e., it should exhibit the same asymptotic behaviour as the strong-coupling anti-adiabatic HMSF). For the  $t$ - $V$  model the analytical form of  $K_\rho$  in the thermodynamic limit is known,

$$K_\rho = \frac{\pi}{2 \arccos[-V/(2t)]}. \quad (10)$$

Hence, the results obtained for  $n(k)$  by DMRG can be fitted by the relation (7), with  $K_\rho$  taken from eq. (10) [37]. Clearly, since eq. (7) is a weak-coupling result, the DMRG data for  $n(k)$  are fitted almost perfectly for small  $V$ . This is demonstrated by figures 3 (a) and (b). Figure 3 (c) shows that the agreement becomes worse for larger Coulomb interaction ( $V = 1.9$ ). In the insulating phase ( $V > 2$ ), the power-law singularity does not exist anymore [c.f. the smooth curves in figure 3 (d)]. As  $V \rightarrow \infty$ , the system becomes a “perfect” CDW, and consequently  $n(k) = 1/2$  for all momenta  $k$ . De facto this situation is realized for  $V = 1000$  already where, according to figure 3 (d),  $n(k)$  is almost constant.

Turning now to the HMSF, we discuss at first the case of large phonon frequencies. Figure 4 gives the  $n(k)$  DMRG data obtained for  $\omega_0 = 10$  (symbols). Obviously, the momentum distribution is a monotonously decreasing function as  $k$  changes from the centre ( $k = 0$ ) to the boundary of the Brillouin zone ( $k = \pi$ ), with a power-law singularity at  $k = k_F$  in the metallic phase [panels (a) to (c)]. Quite different from the  $t$ - $V$  model, however, the momentum distribution becomes renormalised for all momenta  $k$ , as soon as the EP coupling is switched on, where  $n(k)$  decreases (increases) almost uniformly for  $0 \leq k < \pi/2$  ( $\pi/2 < k \leq \pi$ ). Although there is no jump in  $n(k)$  at  $k_F$ , as for an ordinary Fermi liquid, for finite TLL systems

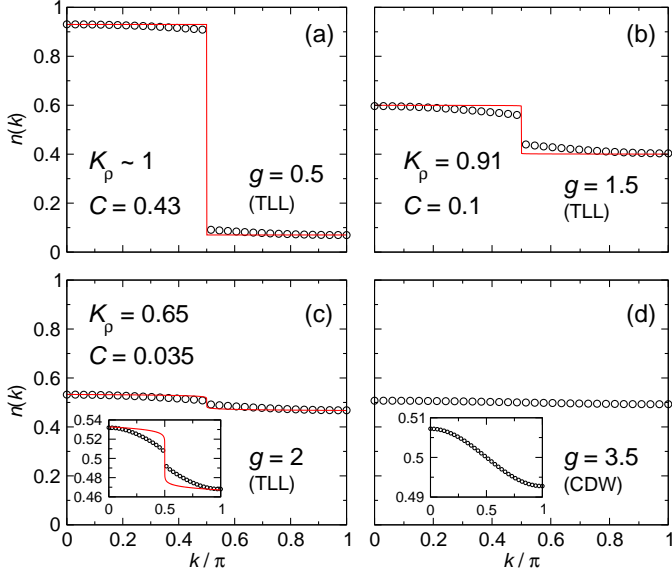


Fig. 4: (Colour online) Momentum distribution function  $n(k)$  in the anti-adiabatic regime ( $\omega_0 = 10$ ) of the half-filled spinless Holstein model. Lines are a fit to eq. (7) with  $K_\rho$  calculated by the DMRG. Insets give  $n(k)$  with magnified axis of ordinate.

the difference  $\Delta = n(k_F - \delta) - n(k_F + \delta)$  is finite (with  $\delta = \pi/N = \pi/66$  in our case), and rapidly decreases with increasing EP interaction  $g$ . As can be seen from the solid lines in figure 4 (a)-(c), the momentum distribution can be surprisingly well fitted to the weak-coupling result (7), just by adjusting the constant  $C$ . Thereby we take the  $K_\rho$ -values extracted from equation (5). Of course, around  $k \simeq k_F$  the agreement becomes worse as  $g$  increases, but we observe a power-law singularity even close to the CDW transition point. Approaching the insulating CDW state this singularity vanishes, and  $\Delta \rightarrow 0$  as  $g \rightarrow g_c$  [cf. the insets in panels (c) and (d)]. In the CDW phase,  $n(k) \simeq 1/2$  for all  $k$  [see panel (d)]. In the anti-adiabatic regime, the CDW state basically constitutes a polaronic superlattice, i.e. the electrons are heavily dressed by phonons and, in addition, ordered in a A-B-structure. Since the polarons are self-trapped, the system tends to be a perfect CDW, as in the limit  $V \rightarrow \infty$  of the  $t$ - $V$  model.

Finally, we investigate the behaviour of  $n(k)$  in the adiabatic regime of the HMSF (see figure 5 for  $\omega_0 = 0.1$ ). In this case,  $n(k)$  is well approximated by equation (7) with  $C = 0.5$  for all  $g < g_c$  [see panels (a) and (b)]. This means the weak-coupling result  $K_\rho \lesssim 1$ ,  $\Delta \lesssim 1$ , holds in (almost) the entire metallic region, where the system can be considered as to be composed of nearly free electrons. The momentum distribution starts to deviate from equation (7) just in the neighbourhood of the metal insulator transition point  $g \simeq g_c$ , but even there  $n(k)$  differs near  $k \sim k_F = \pi/2$  only. Note that  $\Delta$  ( $C$ ) is still very large in the transition region. Of course, very close to the critical point, where a strong renormalisation of  $K_\rho$  takes place (indicating the formation of a TLL with

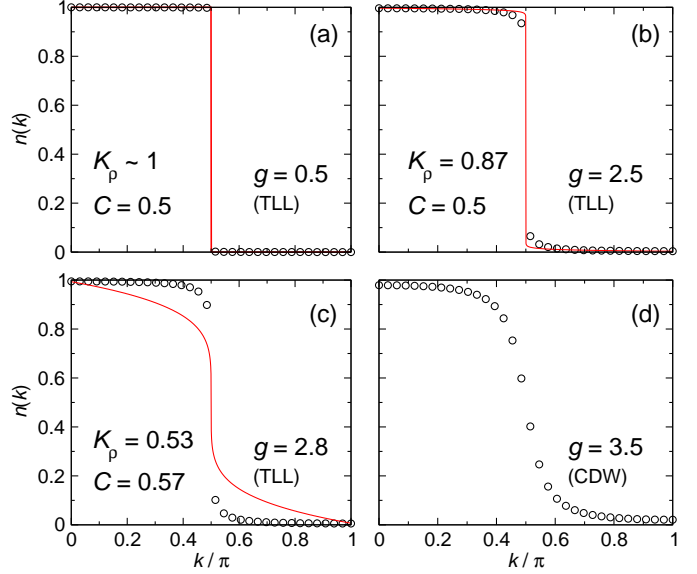


Fig. 5: (Colour online) Momentum distribution function  $n(k)$  in the adiabatic regime ( $\omega_0 = 0.1$ ) of the half-filled spinless Holstein model. Lines are a fit to eq. (7) with  $K_\rho$  calculated by the DMRG.

strong repulsive interactions), the fit of our DMRG data to the weak-coupling relation (7) fails. In the insulating state,  $n(k)$  is given by a smooth curve (without power-law singularity), which – in contrast to the anti-adiabatic case – exhibits a significant curvature because the EP coupling used in figure 5 (d) is small if compared to the half electronic bandwidth  $2t$ .<sup>5</sup> Therefore system now typifies rather a Peierls band insulator than a polaronic superlattice.

To summarise, we investigated the properties of the metallic phase and the metal insulator transition in the spinless fermion Holstein model by means of a boson pseudo-site DMRG technique supplemented by a careful finite-size scaling analysis. In particular we determined the Tomonaga-Luttinger correlation exponent  $K_\rho$  from the long-wavelength limit of the static charge structure factor. This approach yields reliable data for  $K_\rho$  in the whole range of electron-phonon interaction strengths  $g$  and phonon frequencies  $\omega_0$ . We compare our results with new and previous data extracted in an alternative way from leading-order scaling relations for the ground-state energy and single-particle excitation gap. In striking contrast to the latter data we find  $K_\rho < 1$  for all phonon frequencies, i.e., the metallic state of the HMSF represents a repulsive Tomonaga-Luttinger liquid, even in the adiabatic regime. Therefore we conclude that in one dimension we have to include the spin degrees of freedom [7, 8, 15] in order to obtain e.g. a phase with attractive interactions ( $K_\rho > 1$ ), or even dominant superconducting correlations.

<sup>5</sup>Recall that in the adiabatic regime  $\lambda = g^2\omega_0/2t$  is the appropriate dimensionless EP interaction parameter in order to discriminate weak ( $\lambda \ll 1$ ) and strong coupling ( $\lambda \gg 1$ ) situations.

Furthermore, since the metal insulator phase boundary in the  $g\text{-}\omega_0^{-1}$  plane obtained from the  $K_\rho(g, \omega_0) = 1/2$  line is in excellent agreement with previous results [13, 14, 18], we suppose that the TLL-CDW transition in the HMSF is always of Kosterlitz-Thouless type. Comparing the behaviour of the momentum distribution function with the weak-coupling TLL result reveals, however, significant differences regarding the nature of the metallic and insulating phases in the adiabatic and anti-adiabatic regimes of the HMSF. Whereas the metallic state is a weakly renormalised TLL and the CDW phase typifies a Peierls band insulator at small phonon frequencies, a polaronic metal and a polaronic superlattice are formed at large phonon frequencies. This is in accord with the electron and phonon spectral properties detected in Refs. [14, 29]. In the strong-coupling anti-adiabatic regime the momentum distribution function indicates perfect CDW behaviour as in the  $V \rightarrow \infty$  limit of the  $t\text{-}V$  model.

\*\*\*

The authors would like to thank G. Hager, E. Jeckelmann, V. Meden, and S. Nishimoto for valuable discussions. This work was supported by SFB 652.

#### REFERENCES

- [1] PLOOG K. H. and NÖTZEL R. (EDS.), *New Concepts to fabricate semiconductor quantum wire and quantum dot structures* Vol. 419 of *Lecture Notes in Physics* (Springer-Verlag, Berlin/Heidelberg) 1985.
- [2] ISHIGURO T., YAMAJI K. and SAITO G., *Organic Superconductors* (Springer-Verlag, New York) 1973; TSUDA N., NASU K., YANASE A. and SIRATORI K., *Electronic Conduction in Oxides* (Springer-Verlag, Berlin) 1991; BISHOP A. R. and SWANSON B. I., *Los Alamos Sciences*, **21** (1993) 133; HASE M., TERASAKI I. and UCHINOKURA K., *Phys. Rev. Lett.*, **70** (1993) 3651; WELLEIN G., FEHSKE H. and KAMPF A. P., *Phys. Rev. Lett.*, **81** (1998) 3956; TOYOTA N., LANG M. and MÜLLER J., *Low-dimensional molecular metals* (Springer-Verlag, Berlin/Heidelberg) 2007.
- [3] MOTT N. F., *Metal-Insulator Transitions* (Taylor & Francis, London) 1990; MONCEAU P., *Fiz. Tver. Tel.*, **41** (1999) 759.
- [4] PEIERLS R., *Quantum theory of solids* (Oxford University Press, Oxford) 1955; GRÜNER G., *Density Waves in Solids* (Addison Wesley, Reading, MA) 1994.
- [5] TAKADA Y. and CHATTERJEE A., *Phys. Rev. B*, **67** (2003) 081102(R).
- [6] FEHSKE H., WELLEIN G., HAGER G., WEISSE A. and BISHOP A. R., *Phys. Rev. B*, **69** (2004) 165115; FEHSKE H., HAGER G. and JECKELMANN E., *Europhys. Lett.*, **84** (2008) 57001.
- [7] CLAY R. T. and HARDIKAR R. P., *Phys. Rev. Lett.*, **95** (2005) 096401; HARDIKAR R. P. and CLAY R. T., *Phys. Rev. B*, **75** (2007) 245103.
- [8] TEZUKA M., ARITA R. and AOKI H., *Phys. Rev. Lett.*, **95** (2005) 226401; TEZUKA M., ARITA R. and AOKI H., *Phys. Rev. B*, **76** (2007) 155114.
- [9] GIAMARCHI T., *Quantum Physics in One Dimension* (Oxford University Press, Oxford) 2003.
- [10] LUTTINGER J. M., *J. Math. Phys.*, **4** (1963) 1154.
- [11] VOIT J., *Rep. Prog. Phys.*, **58** (1995) 977.
- [12] HOLSTEIN T., *Ann. Phys. (N.Y.)*, **8** (1959) 325; HOLSTEIN T., *Ann. Phys. (N.Y.)*, **8** (1959) 343.
- [13] FEHSKE H., HOLICKI M. and WEISSE A., *Advances in Solid State Physics*, **40** (2000) 235; WEISSE A. and FEHSKE H., *Phys. Rev. B*, **58** (1998) 13526.
- [14] HOHENADLER M., WELLEIN G., BISHOP A. R., ALVERMANN A. and FEHSKE H., *Phys. Rev. B*, **73** (2006) 245120.
- [15] HIRSCH J. E. and FRADKIN E., *Phys. Rev. Lett.*, **49** (1982) 402; HIRSCH J. E. and FRADKIN E., *Phys. Rev. B*, **27** (1983) 4302.
- [16] ZHENG H., FEINBERG D. and AVIGNON M., *Phys. Rev. B*, **39** (1989) 9405.
- [17] MCKENZIE R. H., HAMER C. J. and MURRAY D. W., *Phys. Rev. B*, **53** (1996) 9676.
- [18] BURSILL R. J., MCKENZIE R. H. and HAMER C. J., *Phys. Rev. Lett.*, **80** (1998) 5607.
- [19] SYKORA S., HÜBSCH A., BECKER K. W., WELLEIN G. and FEHSKE H., *Phys. Rev. B*, **71** (2005) 045112.
- [20] KOSTERLITZ J. M. and THOULESS D. J., *J. Phys. C*, **6** (1973) 1181.
- [21] HALDANE F. D. M., *Phys. Rev. Lett.*, **45** (1980) 1358.
- [22] TOMONAGA S., *Prog. Theor. Phys.*, **5** (1950) 544.
- [23] CARDY J. L., *J. Phys. A*, **17** (1984) L385.
- [24] FRAHM H. AND KOREPIN V. E., *Phys. Rev. B*, **42** (1990) 10553; KAWAKAMI N. AND YANG S. K., *Phys. Lett. A*, **148** (1990) 359.
- [25] OGATA M., LUCHINI M. U., SORELLA S., AND ASSAAD F. F., *Phys. Rev. Lett.*, **66** (1991) 2388.
- [26] WEISSE A., FEHSKE H., WELLEIN G. and BISHOP A. R., *Phys. Rev. B*, **62** (2000) R747; FEHSKE H., WELLEIN G., HAGER G., WEISSE A., BECKER K. W. and BISHOP A. R., *Physica B*, **359–361** (2005) 699.
- [27] FIRSOV Y. A., *Polarons* (Izd. Nauka, Moscow) 1975.
- [28] FEHSKE H. and TRUGMAN S. A., *Numerical solution of the Holstein polaron problem* in *Polarons in Advanced Materials*, edited by ALEXANDROV A. S., Vol. 103 of *Springer Series in Material Sciences* (Canopus/Springer Publishing, Dordrecht) 2007 pp. 393–461.
- [29] SYKORA S., HÜBSCH A. and BECKER K. W., *Europhys. Lett.*, **76** (2006) 644.
- [30] EJIMA S., GEBHARD F. and NISHIMOTO S., *Europhys. Lett.*, **70** (2005) 492.
- [31] EJIMA S., HAGER G. and FEHSKE H., *Phys. Rev. Lett.*, **102** (2009) 106404.
- [32] CLAY R. T., SANDVIK A. W. and CAMPBELL D. K., *Phys. Rev. B*, **59** (1999) 4665.
- [33] WHITE S. R., *Phys. Rev. Lett.*, **69** (1992) 2863; JECKELMANN E. and WHITE S. R., *Phys. Rev. B*, **57** (1998) 6376; JECKELMANN E. and FEHSKE H., *Rivista del Nuovo Cimento*, **30** (2007) 259.
- [34] MATTIS D. C. AND LIEB E. H., *J. Math. Phys.*, **6** (1965) 304.
- [35] SÓLYOM J., *Adv. Phys.*, **28** (1979) 201; OGATA M. and SHIBA H., *Phys. Rev. B*, **41** (1990) 2326; PRUSCHKE T. and SHIBA H., *Phys. Rev. B*, **44** (1991) 205.
- [36] QIN S., LIANG S., SU Z. and YU L., *Phys. Rev. B*, **52** (1995) 5475.
- [37] MEDEN V., METZNER M., SCHOLLWÖCK U., SCHNEIDER O., STAUBER T., AND SCHÖNHAMMER K., *Eur. Phys. J. B*, **16** (2000) 631.